UDC 533.98:539.216:620.172.24

**K.H. AHARONYAN**, **A.Zh. KHACHATRIAN**, **E.P. KOKANYAN**

# SCREENED IMPURITIES IN THE FOUR-LAYER MOS SYSTEM

In the inversion channel of the four-layer MOS system, the screened impurity Coulomb interaction potential properties are discussed. An explicit dependence of the effective screening parameter on the thicknesses of the passivation and oxide barrier layers, on their dielectric constants and the 2D EG carrier density is received. The typical physical results such as: a) enhancement of 2D EG carrier screening saturation effect, b) the dependence of the screening mechanism nature on the low-κ and high-κ types of the barrier dielectric layers are established and numerically analyzed.

***Keywords:*** four-layer MOS system, screened potential, effective screening parameter.

Further optimization of the metal-oxide-semiconductor (MOS) system devices currently insists on the importance of both semiconductor active channels with the mobile two-dimensional electron gas (2D EG) and dielectric gate layers with the nano-scale equivalent-oxide thickness. In this regard, the III-V group semiconductors and the high – κ dielectric gate oxides are of key interest now [1]. These active channel materials possess a narrow energy band gap favoring itself an appearance of the impurity states being easily generated in the MOS structure.

In a usual MOS system, an active 2D EG channel operates under the static polarization field caused by dielectric mismatch between the structural semiconductor and dielectric layers. In turn, for the dielectric layer nano-scale thickness values (both passivation and oxide) the polarization field induced by metal gate becomes important [2, 3]. Thus, formed by these fields, the static *polarization screening* (*PS*) mechanism actually initiated by the image charges located both in the dielectric and metal gate layers can, together with the 2D *carrier screening* (*CS*) mechanism, considerably convert the Coulomb interaction of the impurity centers in the MOS active channel. So, the impurity states available in the MOS system might be screened and the special conditions are created in these nanostructures to operate with the physical parameters of the screened impurities by the inter-play of the essential parameters such as: *a*) in-plane density of the 2D EG, *b*) the dielectric constants of the semiconductor and oxide layer media, *c*) the nano-scale thicknesses of the oxide layers.

Thus, clarifying the role of the MOS impurity states influenced simultaneously by the *CS and PS mechanisms* is currently fundamental [4]. In the article presented here this problem is elaborated both analytically and numerically.

Let us have the four-layer MOS structure in accordance with Fig. 1 where the region $z \le -(L+D)$ is occupied by the gate metal, the region $-(L+D) < z \le -L$ by the dielectric oxide layer with dielectric constant $\varepsilon_D$ of the thickness $D$, the region $-L < z \le 0$ by the intermediate dielectric passivation layer of the thickness $L$ with dielectric constant $\varepsilon_L$ and the region $0 < z \le \infty$ by the semiconductor substrate with the dielectric constant $\varepsilon_S$. Here the z axis is perpendicular to the gate layer interfaces. In the model under discussion, the $n$ – type 2D EG channel with the average surface density $n_S$ produces the carrier screening of the impurity charge center sited at the point $\rho = 0$, $z = z_0 > 0$ near the semiconductor/oxide heterojunction. The screened Coulomb interaction potential $\varphi(\rho,\ z)$ of the impurity center is related to the Poisson's equation as:

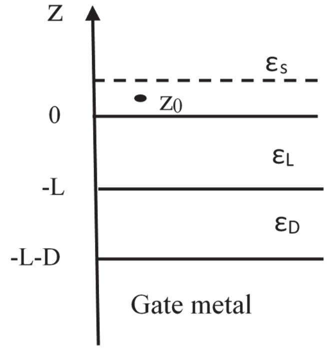

*Fig. The four-layer MOS structure*

$$\varepsilon(z)\nabla_{\vec{r}}^2\, \varphi_s(\vec{r},\vec{r}_0) = -4\pi[e\delta(z-z_0)\delta(\vec{\rho}) + \rho_{ind}(\vec{r},\vec{r}_0)]\,, \qquad (1)$$

where $\delta$ is the Dirac-delta function, $\vec{r} = \vec{r}\ (\vec{\rho}\ , z)$, $\rho$ - the 2D plane coordinate. The solution of Eq.(1) is demonstrated in [5, 6] and in brief looks as:

In Exp (1), $\rho_{ind}$ is the induced charge density, which has the form:

$$\rho_{ind} = -e^2 \frac{\partial n_S}{\partial \mu_0}\, g(z)\, \bar{\varphi}_s(\vec{\rho})\,, \qquad (2)$$

where $\mu_0 >> k_BT$ is the unperturbet chemical potential, $k_BT$ – the energy scale factor, $g(z) = |\psi(z)|^2$ - the normalized charge distribution, $\psi(z\ )$ – the normalized solution of the electrons transverse motion, $\bar{\varphi}_s(\vec{\rho})$– the averaged screened potential as:

$$\bar{\varphi}_s(\vec{\rho}\ , z_0) = \int_0^\infty \varphi_s(\vec{\rho}, z\ , z_0)\ g(z)\ dz\ . \qquad (3)$$

The ratio ( $\partial n_S\ /\partial \mu_0$ ) in Exp.(2) on the condition of the size quantum limit and the electrons essentially confined to move in an active channel plane is:

$$\frac{\partial n_S}{\partial \mu_0} = \frac{m_e}{\pi\hbar^2}\left[1 - \exp\left(-\frac{\pi n_S \hbar^2}{m_e k_B T}\right)\right], \qquad (4)$$

where $m_e$ is the electron effective mass. So Poisson's equation (1) then has the form:

$$\begin{cases} \nabla^2_{\vec{\rho},z}\, \varphi_s(\vec{\rho},z,z_0) - 2q_s g(z)\bar{\varphi}_s(\vec{\rho}\,,z_0) = \frac{-4\pi e}{\varepsilon_s}\delta(\vec{\rho})\delta(z-z_0)\ z \geq 0 \\ \nabla^2_{\vec{\rho},z}\, \varphi_s(\vec{\rho},z,z_0) = 0\ z < 0 \end{cases}, \tag{5}$$

where $q_s$ is the 2D EG screening parameter defined as:

$$q_s = \frac{2\pi e^2}{\varepsilon_s}\frac{\partial n_S}{\partial \mu_0}\,. \tag{6}$$

and for the degenerate and non-degenerate 2D EG statistics takes the forms:

$$q_s = \frac{2}{a_0}\,, (\frac{\pi n_S \hbar^2}{m_e k_B T} >>1) \text{ and } q_s = \frac{2}{a_0}\frac{\pi n_S \hbar^2}{m_e k_B T}\,, (\frac{\pi n_S \hbar^2}{m_e k_B T} <<1)\,. \quad \text{(7a) and (7b)}$$

To solve Eq.(1) for the four-layer MOS system, we utilize the cylindrical coordinate system *ρ, φ,* z, and thus express the interaction potential in Fourier components *φ(k ,z)* with respect to the coordinate $\rho$ as:

$$\varphi_s(\vec{\rho},z,z_0\,) = \frac{1}{(2\pi)^2}\int_0^\infty e^{i\vec{k}\vec{\rho}}\varphi_s(k,z,z_0)\, d^2\vec{k} = \int_0^\infty J_0(k\rho)\varphi_s(k,z,z_0)\, kdk, \tag{8}$$

where $\vec{k}$ is the electron 2D plane vector and $J_0$ - the 0-th order Bessel function.

Applying appropriate boundary conditions for the $\varphi_s(k,z,z_0)$ we have:

$$\varphi_s(k,z\,,z_0)|_{z>0} = \frac{e}{\varepsilon_s}\left[\frac{e^{-k|z-z_0|}}{k} + \frac{\varepsilon_S^* - \varepsilon_O^*}{\varepsilon_S^* + \varepsilon_O^*}\frac{e^{-k(z+z_0)}}{k}\right] -$$

$$-2q_s\bar{\varphi}_s(k,z_0)\int_0^\infty g(z')\, G(z,z')dz', \tag{9}$$

$$G(z,z') = \frac{1}{2k}\left[e^{-k|z-z'|} + \frac{\varepsilon_S^* - \varepsilon_D^*}{\varepsilon_S^* + \varepsilon_D^*}e^{-k(z+z')}\right]$$

and

$$\bar{\varphi}_s(k,z_0) = \int_0^\infty \varphi_s(k,z\,,z_0)|_{z>0}\, g(z)\, dz =$$

$$= \frac{e}{\varepsilon_s}\frac{\left[\int_0^\infty e^{-k|z-z_0|}g(z)\, dz + \frac{\varepsilon_S^* - \varepsilon_O^*}{\varepsilon_S^* + \varepsilon_O^*}\int_0^\infty e^{-k(z+z_0)}\, g(z)\, dz\right]}{k+q_s\left[\int_0^\infty g(z)\, dz\int_0^\infty e^{-k|z-z'|}\, g(z')\, dz' + \frac{\varepsilon_S^* - \varepsilon_O^*}{\varepsilon_S^* + \varepsilon_O^*}\left(\int_0^\infty e^{-kz}\, g(z)\, dz\right)^2\right]}, \tag{10}$$

where $\varepsilon_S^*$ and $\varepsilon_O^*$ are determined by

$$\begin{bmatrix} \varepsilon_S^* = \varepsilon_S\varepsilon_L \sinh(kD)\cosh(kL) + \varepsilon_S\varepsilon_D \cosh(kD)\sinh(kL) \\ \varepsilon_O^* = \varepsilon_L^2 \sinh(kD)\sinh(kL) + \varepsilon_L\varepsilon_D \cosh(kD)\cosh(kL) \end{bmatrix}. \tag{11}$$

Exps. (9) and (10) present the screened Coulomb interaction potential Fourier component related to the active channel region of the four-layer MOS structure.

Here we take an active channel carrier's strong quantum confinement (QC) regime in accordance with the conditions $a_0$ >> *d*, $r_D$ >> *d*, where $a_0 = \varepsilon_S\hbar^2/m_e e^2$

and $r_D$- are correspondingly the effective Bohr and Debye radii in the bulk semiconductor, $d$ - is the active layer effective thickness. The parameter $d/a_0$ determines the criterion of two-dimensionality of the problem and for that 2D EG should be dense and so weakly nonideal [2]. To the latter in size quantum limit corresponds the condition $n_s a_0^2 >> 1$, i.e. the number of surface electrons on the area of the Bohr orbit should be large.

Under these circumstances in Exps. (9) and (10), an important role will be played by 2D distances of $\rho >> d$, for there exists, in the 2D, a wave vector $k$ interval, so that $k\,d << 1$. So the conditions $k\,z << 1$ and $k\,z_0 << 1$ have to be imposed, which permits in the leading order of the parameter $d/a_0$ to get a solution of Eq.(9) as:

$$\varphi_S(k)|_{z>0} = \frac{e}{\varepsilon_S} \frac{1}{\frac{\varepsilon_S^* + \varepsilon_O^*}{2\varepsilon_S^*}k + q_S} \,. \tag{12}$$

Since the realistic MOS devices possess sufficiently thin passivation and thin oxide gate layers, Exp.(12) should be modified in accordance with the long wave related conditions $kL << 1$, $kD < 1$. The result leads the Exp. (12) to the form:

$$\varphi_S(k)|_{z>0} = \frac{2e}{\varepsilon_S} \frac{1}{k + q_S^*}, \tag{13}$$

where

$$q_S^* = 2q_S + \frac{\varepsilon_D \varepsilon_L}{\varepsilon_S(\varepsilon_D L + \varepsilon_L D)}. \tag{14}$$

is the screening parameter formed jointly by the *CS* and *PS* mechanisms.

With the real–space interaction energy $V_s(\rho) = -e\varphi(\rho)$ is:

$$V_S(\rho) = -\frac{2e^2}{\varepsilon_S}\left\{\frac{1}{\rho} - \frac{\pi}{2} q_S^* [H_0(q_S^*\rho) - N_0(q_S^*\rho)]\right\}, \tag{15}$$

where *H(x)* and *N(x)* are the Struve and Neumann functions.

Exp.(15) holds the same $k$ - and $\rho$ - dependences as the corresponding value in the MOS structure with the bulk dielectric layer [2, 3] but is characterized by the more general effective screening parameter $q_S^*$, which depends simultaneously on the key physical parameters of the 2D EG and dielectric layers ($n_s$, $\varepsilon_S$, $\varepsilon_D$, $\varepsilon_L$, $L$, $D$).

Exp. (15) generalizes the previously derived screening parameter expressions concerning the *CS* (first term in Exp.(15)), as well as the *PS* mechanisms (second term in Exp.(14)), respectively. It is distinctive that in $q_S^*$ , the contributions being produced by the aforementioned screening mechanisms are characterized by the additive terms. The nano-scale thickness of the oxide layer leads to the related term in the effective screening parameter $q_S^*$ as $q_S^*|_{PS} = \frac{\varepsilon_D \varepsilon_L}{\varepsilon_S(\varepsilon_D L + \varepsilon_L D)}$ and the correlation of which with the CS mechanism the responsible term ($q_S^*|_{CS} = 2q_S$) actually leads to the characteristic physical consequences:

1) enhancement of the carrier saturation effect specific of the 2D EG screening,

2) dependence of the screening mechanism nature (*PS* and *CS*) on the dielectric types of the passivation and oxide layers.

As we can see from Exps. (14) and (15), with the mutual layout of the material parameters of the passivation and oxide layers, it is possible to manipulate with the nature of the screening mechanism, i.e. to implement a design of the screened impurity interaction in the MOS structure. This can be achieved by using the gate layers of different nano-scale thicknesses with different dielectric types from one side and simultaneously applying the appropriate 2D EG type (degenerate or non-degenerate) on the other side.

Let us now consider numerically the background impurity ground state key parameter such as 2D EG effective screening parameter depending on the nature of the screening in a given structure. Proceeding from the analytical form of Exp. (14) we will rely on the realistic model based on the InSb high mobility active medium with the smallest electron effective mass ($m^* \approx 0.014 m_0$ , $m_0$ - is the free electron mass)) and a macroscopically large impurity effective Bohr radius ($a_0 \approx 64.1$ nm) since for this a criterion of the two-dimensionality of the problem is fully satisfied.

Our calculations were performed on the basis of the real nano-scale thickness dielectric layer MOS structure, namely, *InSb/S(sulfur)/HfO$_2$/metal* [7] with the the low-κ/high-κ dielectric contact (*lh*- κ type MOS structure).

In particular, the numerical results of the effective screening parameter $q_S^*$ , the ($q_S^*|_{PS}$ , $q_S^*|_{CS}$ ) contributions in the $q_S^*$ as the function of the oxide nano-scale thickness $D \in (1.5 \div 8\ nm)$ with the characteristic two $n_s/T$ parameter values $n_s/T\,|_a \approx 6.6.10^7\ cm^{-2}/{}^0K$ ***as the case a)*** and $n_s/T\,|_b \approx 6.6.10^8\ cm^{-2}/{}^0K$ ***as the case b)*** are demonstrated.

For these cases, the 2D EG statistic parameter $\frac{\pi n_S \hbar^2}{m_e k_B T}$ takes the values as $\frac{\pi n_S \hbar^2}{m_e k_B T} \approx 0.13$ and $\frac{\pi n_S \hbar^2}{m_e k_B T} \approx 1.3$, i.e. the *CS* mechanism is provided here correspondingly by the non-degenerate and near-degenerate types of 2D EG. Along with the cases *a*) and *b*), the contributions of the PS and CS mechanisms to $q_S^*$ ($q_S^*|_{PS}$ , $q_S^*|_{CS}$ ) for the degenerate 2D EG ($n_s/T\,|_c \approx 6.6.10^9\ cm^{-2}/{}^0K$) ***as the case c)*** are clarified as well.

*Table*

*The numerical results of the $q_S^*$ , $q_S^*|_{PS}$ and $q_S^*|_{CS}$ parameter values with the* **$n_s/T|_a \approx 6.6.10^7$ $cm^{-2}/^0K$ , $n_s/T|_b \approx 6.6.10^8$ $cm^{-2}/^0K$ , $n_s/T|_b \approx 6.6.10^9$ $cm^{-2}/^0K$** *parameter values for the InSb/S/HfO$_2$ (lh- κ type) MOS structure*

| $\frac{n_S}{T}$ ($cm^{-2}/K$) | D (nm) | $\frac{n_S}{T}\Big\|_{PS}$ ($cm^{-2}/K$) | $q_S^*$ ($nm^{-1}$) | $\frac{q_S^*\|_{PS}}{q_S^*}$ (%) | $\frac{q_S^*\|_{CS}}{q_S^*}$ (%) |
|---|---|---|---|---|---|
| **a) $n_s/T|_a \approx 6.6.10^7$** | 2 | $6.9.10^8$ | $9.6.10^5$ | 92 | 8 |
| | 8 | $5.1.10^8$ | $7.1.10^5$ | 89 | 11 |
| **b) $n_s/T|_b \approx 6.6.10^8$** | 2 | $6.9.10^8$ | $1.32.10^6$ | 65 | 35 |
| | 8 | $5.1.10^8$ | $1.1.10^6$ | 58 | 42 |
| **c) $n_s/T|_c \approx 6.6.10^9$** | 2 | $6.9.10^8$ | $1.48.10^6$ | 58 | 42 |
| | 8 | $5.1.10^8$ | $1.26.10^6$ | 50 | 50 |

Herewith, based on the real case from the Ref.7, the thickness of the passivation layer is taken *L= 1nm* and for the values of the oxide layer dielectric constants have: $\varepsilon_S|_{InSb} \approx 16.9$, $\varepsilon_L|_S \approx 1$, $\varepsilon_D|_{HfO2} \approx 25$. As follows, we have correspondingly the low-κ and high-κ passivation and oxide layers in the MOS. As shown in Table 1, in all cases under discussion, the *PS* mechanism becomes predominant which is quite expected connected with the presence of the high-κ type oxide layer. In this regard, a stronger saturation effect for a non-degenerate 2D EG takes place (sub-table *1a*).

At the same time, for the degenerate 2D EG (sub-table *1c*), starting only at the large values with *D=8nm* the balance between the *PS* and *CS* mechanisms becomes equal whereas in the first case this happens already from the *D=3.75nm* oxide thickness value (sub-table *1c*). As follows, the presence of the oxide layer with high-κ type here leads to a complete dominance of the *PS* mechanism in relation to the *SC* mechanism in the effective screening parameter $q_S^*$ regardless of the increase in the 2D EG $n_s/T$ parameter.

## REFERENCES

1. Demonstrating 1 nm-oxide-equivalent-thickness HfO2/InSb structure with unpinning Fermi level and low gate leakage current density / **H.-D. Trinh, et al** // Appl.Phys. Lett.- 2013.-V.103.- P.142903-1-5.
2. **Chaplik A.V.** Possible crystallization of charge carriers in low-dimensional inversion layers // Sov. Phys. JETP. - 1972.-V.35.-P.395.
3. **Aharonyan K.H., Kazaryan E.M., Kokanyan E.P**. Coulomb interaction in the finite dielectric environment based MOSFET structures // Semiconductor Micro- and Nanoelectronics, 11th Int. Conf. -Yerevan.-2017.-P. 41.

4. **Konar A., Bajaj M., Pandey R.K., Murali K.V.R.M.** Dielectric environment mediated quantum screening of two-dimensional electron gas// J. of Appl. Phys.- 2013.-V.114.-P.113707-1-6.
5. **Stern F., Howard W.E.** Properties of Semiconductor Surface Inversion Layers in the Electric Quantum Limit// Phys. Rev.-1967.-V.163.-P. 816.
6. **Averkiev N.S.**, **Pikus G.E.**, **Shmatov M.L.** Surface excitons and acceptors in MOS structures// Sov. Phys. - Solid State.-1988.-V. 30.-P. 1844].
7. U.S. Patent Dielectric interface for group III-V semiconductor device /**J.K. Brask, et al**.-2009.-No.7485503 B2.-P.1.

## Կ.Հ. ԱՀԱՐՈՆՅԱՆ, Ա.Ժ. ԽԱՉԱՏՐՅԱՆ, Է.Պ. ԿՈԿԱՆՅԱՆ

## ԷԿՐԱՆԱՎՈՐՎԱԾ ԽԱՌՆՈՒԿՆԵՐԸ ՔԱՌԱՇԵՐՏ ՄՕԿ ՀԱՄԱԿԱՐԳՈՒՄ

ՄՕԿ քառաշերտ համակարգի ինվերսիոն շերտում քննարկված են էկրանավորված խառնուկի կուլոնյան փոխազդեցության պոտենցիալի հատկությունները: Ստացված է արդյունարար էկրանավորման պարամետրի բացահայտ կախվածությունը պասսիվացման և օքսիդային արգելքային շերտերի հաստություններից, դիէլեկտրիկական հաստատուններից և 2Չ ԷԳ լիցքերի խտությունից: Հաստատված են բնորոշ ֆիզիկական արդյունքներ, ինչպիսիք են՝ ա) 2Չ ԷԳ լիցքերով էկրանավորման հագեցման երևույթի ուժեղացումը, բ) էկրանավորման մեխանիզմի բնույթի կախվածությունը արգելքային շերտերի դիէլեկտրական տիպից (բարձր- և ցածր- к), որոնք նաև ենթարկված են թվային վերլուծության:

***Առանցքային բառեր.*** ՄՕԿ քառաշերտ համակարգ, էկրանավորման պոտենցիալ, էկրանավորման արդյունարար պարամետր:

## К.Г. АГАРОНЯН, А.Ж. ХАЧАТРЯН, Е.П. КОКАНЯН

## ЭКРАНИРОВАННЫЕ ПРИМЕСИ В ЧЕТЫРЕХСЛОЙНОЙ МОП СИСТЕМЕ

В инверсионном канале четырехслойной системы металл-оксид полупроводник (МОП) обсуждаются свойства потенциала кулоновского взаимодействия экранированной примеси. Получена явная зависимость эффективного параметра экранирования от толщин пассивационного и оксидного барьерных слоев, диэлектрических проницаемостей и от плотности носителей 2М ЭГ. Установлены характерные физические результаты, такие как: а) усиление эффекта насыщения экранирования при 2М ЭГ; б) зависимость природы механизмов экранирования от диэлектрических типов (с высоким- и низким- к) барьерных диэлектрических слоев, которые также численно проанализированы.

***Ключевые слова:*** четырехслойная МОП система, экранированный потенциал, эффективный параметр экранирования.